Weed Science

www.cambridge.org/wsc

Enhancing image recognition robustness in early weed detection through optimal training data curation

Saeko Matsuhashi[1], Yu Oishi[2], Akira Koarai[3] and Ryo Sugiura[4]

[1]Senior Scientist, Institute for Plant Protection, National Agriculture and Food Research Organization (NARO), Tsukuba, Ibaraki, Japan; [2]Principal Scientist, Research Center for Agricultural Information Technology, NARO, Tsukuba, Ibaraki, Japan; [3]Division Manager, Institute for Plant Protection, NARO, Tsukuba, Ibaraki, Japan and [4]Unit Leader, Research Center for Agricultural Information Technology, NARO, Memuro, Hokkaido, Japan

Research Article

Cite this article: Matsuhashi S, Oishi Y, Koarai A, Sugiura R (2024) Enhancing image recognition robustness in early weed detection through optimal training data curation. Weed Sci. **72**: 546–552. doi: 10.1017/wsc.2024.63

Received: 31 January 2024
Revised: 11 June 2024
Accepted: 17 July 2024
First published online: 9 October 2024

Associate Editor:
Muthukumar V. Bagavathiannan, Texas A&M University

Keywords:
Alien species; deep learning; site-specific weed management; YOLOv5; VGG19

Corresponding author:
Saeko Matsuhashi;
Email: sae.matsuhashi@gmail.com

Abstract

Using convolutional neural networks (CNNs) for image recognition is effective for early weed detection. However, the impact of training data curation, specifically concerning morphological changes during the early growth phases of weeds, on recognition robustness remains unclear. We focused on four weed species (giant ragweed [*Ambrosia trifida* L.], red morningglory [*Ipomoea coccinea* L.], pitted morningglory [*Ipomoea lacunosa* L.], and burcucumber [*Sicyos angulatus* L.]) with varying cotyledon and true leaf shapes. Creating 16 models in total, we employed four dataset patterns with different growth stage combinations, two image recognition algorithms (object detection: You Look Only Once [YOLO] v5 and image classification: Visual Geometry Group [VGG] 19), and two conditions regarding the number of species treated (four and two species). We evaluated the effects of growth stage training on weed recognition success using two datasets. One evaluation revealed superior results with a single class/species training dataset, achieving >90% average precision for detection and classification accuracy under most conditions. The other dataset revealed that merging different growth stages with different shapes as a class effectively prevented misrecognition among different species when using YOLOv5. Both results suggest that integrating different shapes in a plant species as a single class is effective for maintaining robust recognition success amid temporal morphological changes during the early growth stage. This finding not only enhances early detection of weed seedlings but also bolsters the robustness of general plant species identification.

Introduction

Identification of weed species and their growth stages is critical for devising effective weed management strategies (Rydahl 2003; Teimouri et al. 2018). Moreover, managing weeds during their early growth stages is essential for efficient weed control and sustainable agricultural productivity (Hussain et al. 2021). Early-stage weeds are more easily removed through physical and chemical means, reducing herbicide usage (Espejo-Garcia et al. 2020), costs, and time and labor requirements. However, identifying weeds at early growth stages in crop fields is challenging due to their small size and differences in shape compared with mature plants.

To enhance weed detection, the application of image recognition employing convolutional neural networks (CNNs) is on the rise (Coleman et al. 2022; Hasan et al. 2021; Rai et al. 2023). Automating the process of finding weeds (Lottes et al. 2018; Sujaritha et al. 2017) and mapping their distributions (Huang et al. 2018; Partel et al. 2019) is expected to contribute to the facilitation of site-specific weed management (SSWM; Barnhart et al. 2022; Wang et al. 2019). Despite the accumulation of case studies for practical applications, growth stages have been identified as complicating factors in weed recognition (Coleman et al. 2022), and their effects on the performance of CNN algorithms remain poorly understand (Coleman et al. 2022; Hasan et al. 2021; Wang et al. 2019). Particularly at the early growth stage, there is a possibility that the accuracy of weed recognition is unstable or decreases because the reflectance characteristics of crops and weeds are generally similar (López-Granados 2011; Wang et al. 2019), and the shapes of dicotyledons tend to change markedly during seedling development. Given that cotyledons and true leaves often have different shapes in many species, even humans may struggle to recognize them as the same species without proper knowledge. Teimouri et al. (2018) demonstrated that leaf numbers may be useful for estimating early growth stages with a classification algorithm; however, accuracy tended to vary among stages and species. To apply image recognition to weed management, understanding how changes in plant shape during the early growth stage influence accuracy is essential.

In this study, we address how the change in plant shape during the early growth stage should be incorporated into image recognition training. To address these challenges, we focused on four weed

© The Author(s), 2024. Published by Cambridge University Press on behalf of Weed Science Society of America.

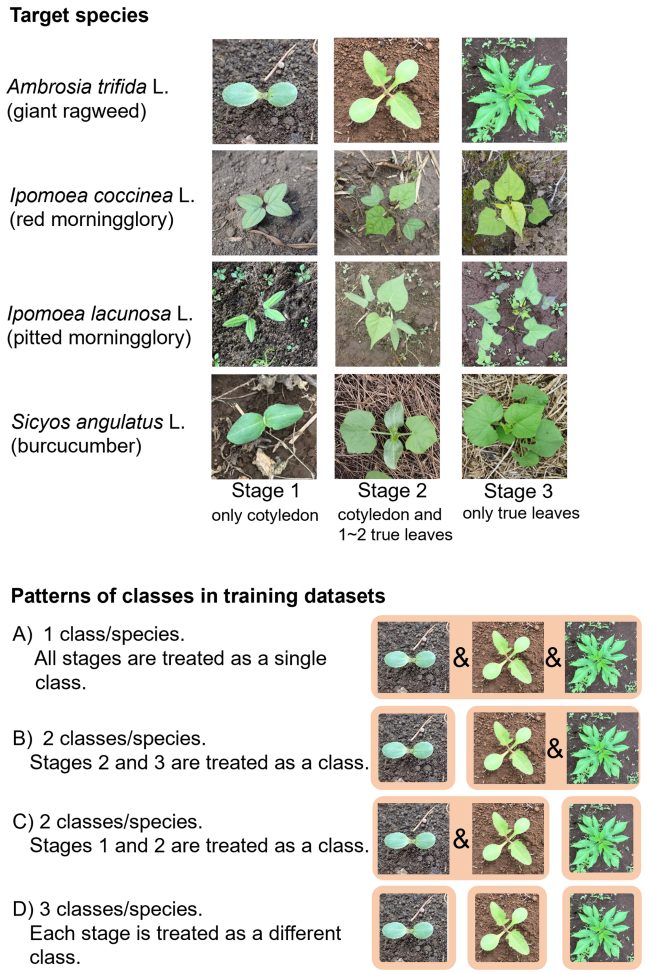


Figure 1. Target species and class patterns used in the training datasets.

species with different cotyledon and true leaf shapes: giant ragweed (*Ambrosia trifida* L.), red morningglory (*Ipomoea coccinea* L.), pitted morningglory (*Ipomoea lacunosa* L.), and burcucumber (*Sicyos angulatus* L.). Each of these species is a major noxious annual in crop fields globally, causing widespread yield loss (Grey and Raymler 2002; Kurokawa et al. 2015; Lee and Son 2022; Norsworthy and Oliveira 2007; Regnier et al. 2016; Savić et al. 2021; Smeda and Weller 2001). In Japan, these species pose a threat to soybeans [*Glycine max* (L.) Merr.] and/or feed grains as invasive alien species (Kurokawa 2017). Notably, *S. angulatus* is designated as a "species to be managed urgently" in "The List of Alien Species That May Have Adverse Effects on Ecosystems in Japan" (Ministry of the Environment, Ministry of Agriculture, Forestry and Fisheries 2015), with its cultivation being banned without permission. By comparing models that use different class patterns in training datasets, we illustrate how to maintain the robustness of recognition accuracy amid temporal morphological changes during the early growth stage.

Materials and Methods

Target Species and Image Acquisition for Training

Leaf shapes of the target species (*A. trifida*, *I. coccinea*, *I. lacunosa*, and *S. angulatus*) exhibit both similarities and differences (Figure 1). Cotyledons in *A. trifida* and *S. angulatus* are round, whereas those in *I. coccinea* and *I. lacunosa* are V-shaped. True

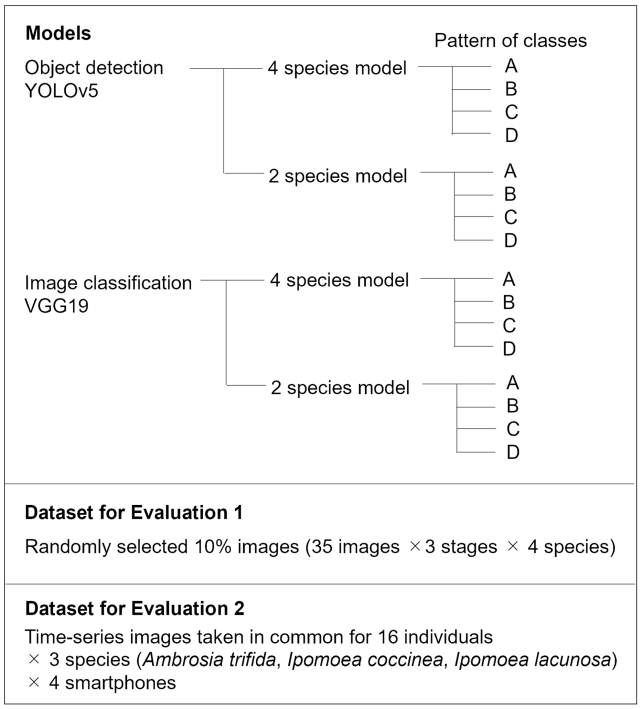


Figure 2. Study design. Note that *Sicyos angulatus* was not used in Evaluation 2, because its cultivation is not permitted in Japan. YOLOv5, You Look Only Once v5; VGG19, Visual Geometry Group 19.

leaves of *I. coccinea*, *I. lacunosa*, and *S. angulatus* are roughly heart-shaped and alternate, whereas those of *A. trifida* are deltate or palmately 2- to 5-lobed and opposite.

Training images were captured in situ using 10 device makers' digital cameras and smartphones in Japan (35.8°N to 37.7°N, 137.9°E to 140.5°E) during April to October in 2019, 2021, and 2022. Images were taken from 5 to 100 cm directly above plants, irrespective of weather and light conditions. These images were categorized into three growth stages (Figure 1): Stage 1, target weeds with only cotyledons; Stage 2, cotyledons and one or two true leaves; and Stage 3, only true leaves. Although some images included non-target plants and/or multiple target plants, each image could be categorized into one stage of one target species. For each stage of each species, 350 images were acquired (350 × 3 stages × 4 species = 4,200 images in total). These images were randomly divided in an 8:1:1 ratio for training, validation, and testing (280, 35, and 35 images/stage/species), respectively. The test data were used for Evaluation 1 (Figure 2). The image area containing the target species was annotated using an open-source tool LabelImg (Tzutalin 2015) for detection models.

Training Datasets

To assess the impact of varying training for growth stages on weed recognition success, we prepared four dataset patterns with different class definitions (Figure 1): (A) one class/species, treating Stages 1, 2, and 3 as a single class; (B) two classes/species, treating Stages 2 and 3 as a class; (C) two classes/species, treating Stages 1 and 2 as a class; and (D) three classes/species, treating each stage as a different class.

To ensure the robustness of the effects among A, B, C, and D, we prepared 16 models using two image recognition algorithms and a

https://doi.org/10.1017/wsc.2024.63 Published online by Cambridge University Press

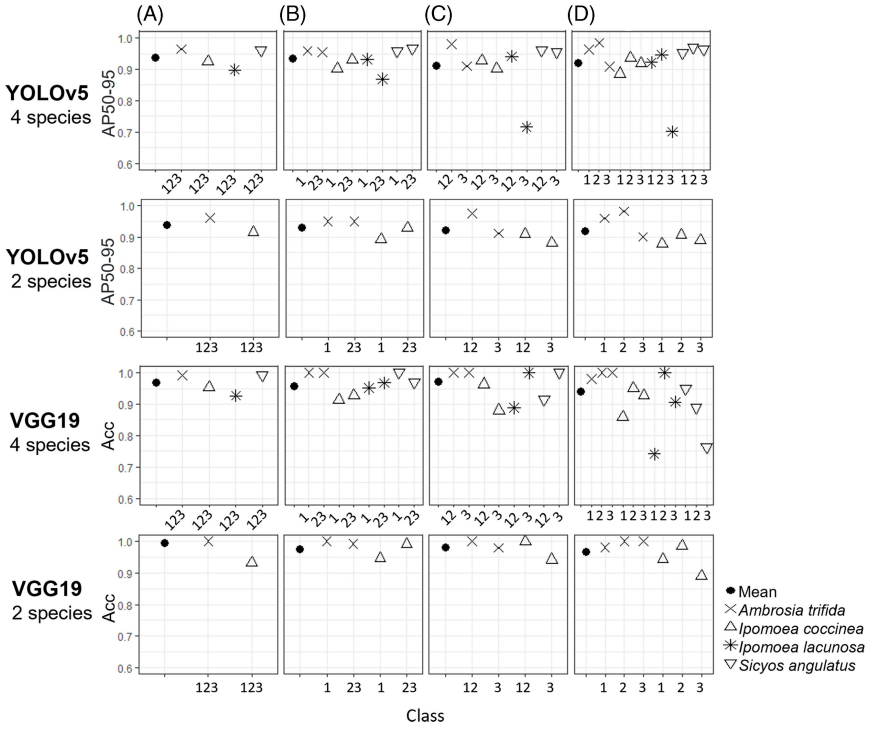


Figure 3. Evaluation 1 results under You Look Only Once [YOLO] v5 and Visual Geometry Group [VGG] 19 for four and two weed species. Each algorithm was applied to four training datasets with different class definitions as follows: (A) one class/species, treating growth Stages 1 (target with only cotyledons), 2 (cotyledons and one or two true leaves), and 3 (only true leaves) as a single class; (B) two classes/species, treating Stages 2 and 3 as a class; (C) two classes/species, treating Stages 1 and 2 as a class; and (D) three classes/species, treating each stage as a different class.

couple of conditions regarding the number of species treated (four and two species) (Figure 2). In the two-species models, we selected *A. trifida* and *I. coccinea*, which exhibit unsimilar leaf shapes throughout all stages.

Model Training

Two prominent open-source algorithms, namely the object detection algorithm You Look Only Once (YOLO) v5 (Jocher 2020) and the classification algorithm Visual Geometry Group (VGG) 19 (PyTorch tutorials: https://pytorch.org/tutorials, accessed: January 23, 2024), were applied to eight training datasets (4 class patterns × 2 species number conditions) within the Python 3.7.16 environment using PyTorch 1.13.1. Both YOLO and VGG are often used for weed recognition studies (Hasan et al. 2021; Rai et al. 2023). Regarding YOLOv5, a YOLOv5s architecture was trained with pretrained weights (yolov5s.pt) of the COCO network (Lin et al. 2014), employing default hyperparameter settings (Jocher 2020). Each model underwent training for up to 200 epochs with 32 images per batch. Regarding VGG19, models were trained for up to 100 epochs with a batch size of 30, using an optimizer with a momentum of 0.9 and a learning rate of 0.001. Proper learning convergence was confirmed for both YOLOv5 and VGG19, and the best weights from each training session were used for subsequent analysis. To evaluate model accuracy for each species, average precision (AP) at 0.5 threshold for intersection over union and classification accuracies were calculated for YOLOv5 and VGG19, respectively, using the abovementioned test dataset and the best weight (Evaluation 1). All training and evaluation were conducted on the NARO AI research supercomputer Shiho, equipped with NVIDIA Tesla V100 SXM2 GPU 32GB (NVIDIA, CA, USA).

Collection and Evaluation of Time-Series Images

To evaluate the accuracy of each model in capturing temporal morphological changes during the early growth stage (Evaluation 2; Figure 2), we collected time-series images. We sowed and cultivated 16 individuals of 3 target weeds, namely *A. trifida*, *I. coccinea*, and *I. lacunosa*, with *S. angulatus* excluded, as its cultivation is not permitted in Japan, at the experimental garden at NARO (Tsukuba, 36.03°N, 140.10°E) during May to June 2023. Images were captured from 30 to 50 cm directly above the plants 2 to 5 d wk^{-1}. To minimize differences in sunlight condition, we used a sunshade during shooting. We recorded the number of true leaves for each plant, with zero true leaves corresponding to Stage 1 and one or two true leaves corresponding to Stage 2. To set replications for each date and plant and ensure data independence from training data, four different smartphones (Apple iPhone SE [Apple, CA, USA], SHARP A103SH [SHARP, Osaka, Japan], FCNT F-41B [FCNT, Kanagawa, Japan], and Samsung SC-56B [Samsung, Gyeonggi-do, Korea]) not used for training data collection were employed. As images taken with the autofocus of three smartphones, excluding the Apple iPhone SE, sometimes exhibited blown-out highlights depending on weather conditions, we set their exposure values to a minimum to avoid this. In total, 3,652 images (14 to 27, 8 to 25, and 14 to 22 per plant per camera for *A. trifida*, *I. coccinea*, and *I. lacunosa*, respectively) were collected.

All images were subjected to inference using YOLOv5 and VGG19 models (Figure 2). Four-species models were applied to all images, and two-species models were applied to images of *A. trifida* and *I. coccinea*. To evaluate changes in accuracy along with growth, we assessed the recognition success of each image rather than using comprehensive indices such as mean AP (mAP) and accuracy. In YOLOv5-based detection, inference results with a confidence

https://doi.org/10.1017/wsc.2024.63 Published online by Cambridge University Press

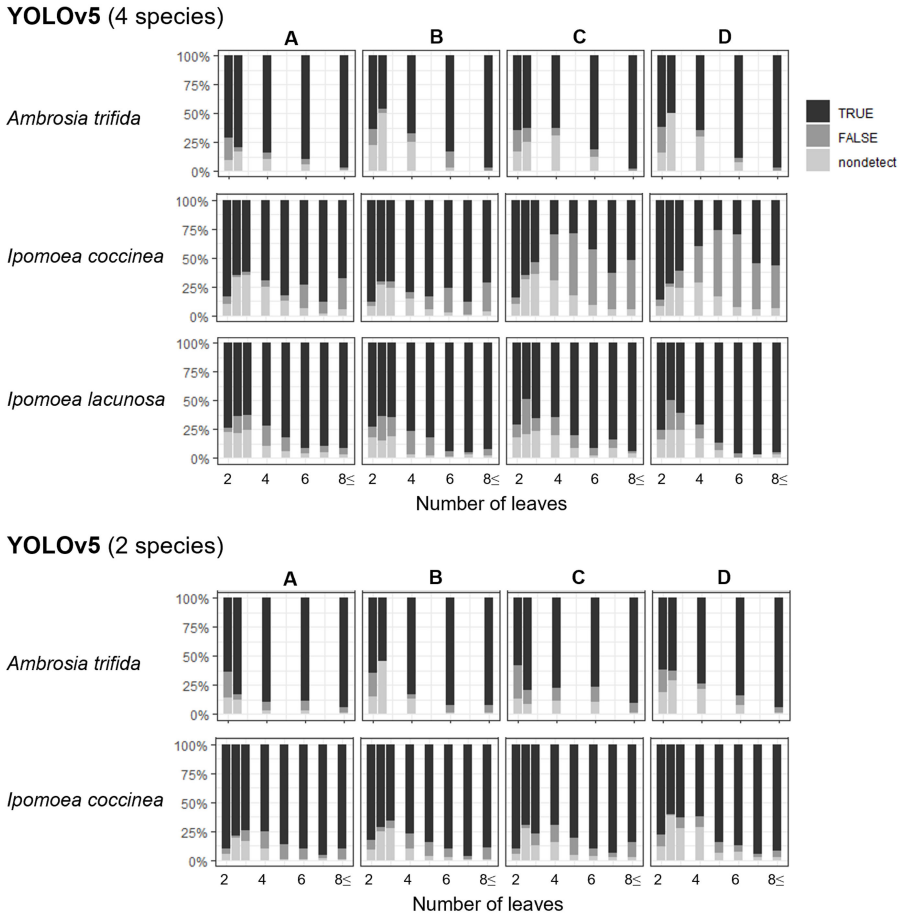


Figure 4. Evaluation 2 time-series detection results under You Look Only Once [YOLO] v5. A, B, C, and D indicate class patterns in training datasets. When the number of leaves is two, this corresponds to Stage 1 (only cotyledons). When the number of leaves is three or four, this corresponds to Stage 2 (cotyledons and one or two true leaves). When the number of leaves is 2.5, this indicates half-grown true leaves. Note that *Sicyos angulatus* was not used in Evaluation 2, because its cultivation is not permitted in Japan.

threshold of 0.5 were defined as "TRUE" (detected only correct species), "FALSE" (results including incorrect species and/or locations), and "NONDETECT." For VGG19-based classification, inference results were defined as TRUE or FALSE as a result was classified to one species per image. When a target's shape displayed intermediate stages, that is, between Stages 1 and 2 or between 2 and 3, both stages (Stages 1 and 2 or 2 and 3) were considered correct. As VGG19 is a classification algorithm and does not indicate where models focused on location in an image, we created heat maps illustrating visual explanations of classification through VGG19 using gradient-weighted class activation mapping (GradCAM; Gildenblat 2021; Selvaraju et al. 2020).

We assessed whether the number of images assigned to TRUE was affected by patterns A, B, C, and D using a generalized linear mixed model with a binomial distribution, employing the *glmer* function from the LME4 package in R v. 4.3.0 (R Core Team 2023). With four replications for each date and plant, the maximum number of TRUE for each date and plant was four. The number of TRUE per four replications was considered the response variable, whereas patterns A, B, C, and D were treated as the explanatory variables, and the plant individual was regarded as the random effect. Separate analyses were conducted for each species, that is, *A. trifida*, *I. coccinea*, and *I. lacunosa*.

Results and Discussion

Comparison of Model Accuracy

Regarding the results of Evaluation 1, the mAP and mean accuracy of pattern A, treating all stages as a single class, surpassed those of the other patterns in most species under both YOLOv5 and VGG19 (Figure 3). Although the AP and accuracy of some classes in B, C, and D were marginally higher than those in A, certain instances in C and D (e.g., *I. lacunosa* in the four-species models under YOLOv5 and VGG19) exhibited a decrease of more than 0.1. When comparing the four-species and two-species models were compared, the AP values of *A. trifida* remained nearly constant under YOLOv5 across patterns A to D. Conversely, the accuracy in two-species models under VGG19 was slightly higher than that in four-species models. These findings suggest that because lower species number in a model contributes to higher accuracy in classification, such as in VGG19, it is necessary to narrow down the number of targets as appropriate.

Regarding four-species models, the AP and accuracy of *I. lacunosa* tended to be lower than those of the other species. Images of *I. lacunosa* were occasionally misrecognized as *I. coccinea* under both YOLOv5 and VGG19. Moreover, images categorized as Stage 3 were sometimes incorrectly detected as

https://doi.org/10.1017/wsc.2024.63 Published online by Cambridge University Press

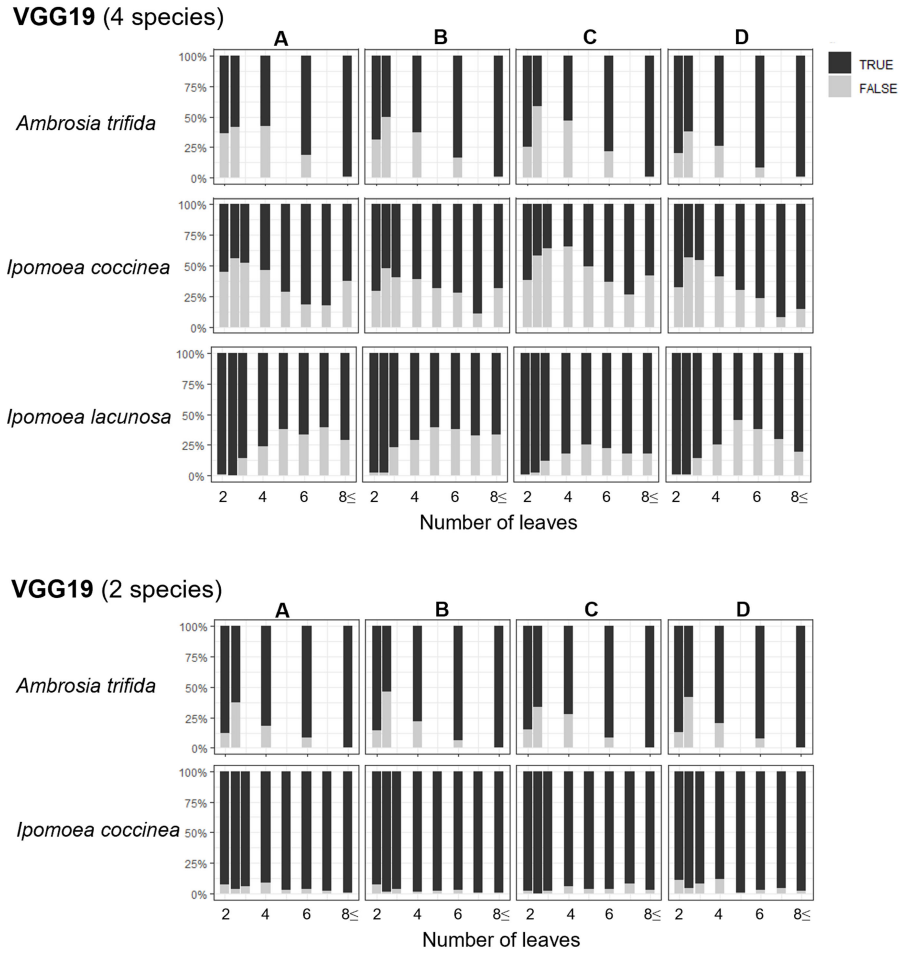


Figure 5. Evaluation 2 time-series detection results under Visual Geometry Group [VGG] 19. A, B, C, and D indicate class patterns in training datasets. When the number of leaves is two, this corresponds to Stage 1 (only cotyledons). When the number of leaves is three or four, this corresponds to Stage 2 (cotyledons and one or two true leaves). When the number of leaves is 2.5, this indicates half-grown true leaves. Note that *Sicyos angulatus* was not used in Evaluation 2, because its cultivation is not permitted in Japan.

nontargets under YOLOv5. During Stage 3, *I. coccinea* typically exhibits more leaf-angle variation compared with the other three species; therefore, capturing its features may be challenging. However, the AP and accuracy of models with patterns A and B, integrating Stage 3 of *I. coccinea* with Stage 1 and/or 2, surpassed those with patterns C and D. This implies that growth stages influence recognition success, although integrating different stages could maintain higher accuracy. Despite the same class number between B and C, the accuracy in B was higher than that in C, suggesting that the combination of integrating growth stages is important to improve accuracy.

Overall, these Evaluation 1 results suggest that integrating growth stage classes for each species, rather than separating classes by growth stages, could contribute to maintaining higher accuracy in both detection and classification. As it is possible that not only class number but also different combinations integrating growth stage classes influence accuracy, optimization is necessary to compare accuracy among these combinations.

Image Recognition Robustness against Temporal Change

In Evaluation 2 results for images depicting temporal morphological changes in *A. trifida*, *I. coccinea*, and *I. lacunosa*, variations in recognition success emerged among species, class patterns, algorithms, and growth stages (Figures 4 and 5). Under YOLOv5, the detection success rate (TRUE detection rate) for *A. trifida* and *I. coccinea* in pattern A tended to surpass that in patterns B, C, and D (Figure 4; Supplementary Table S1). In particular, regarding the four-species model with patterns C and D of *I. coccinea* when the number of true leaves exceeded two (four or more leaves), detection failure increased: true leaves of *I. coccinea* were occasionally misidentified as those of *I. lacunosa* or *S. angulatus*. It is possible that these models could not distinguish shapes and arrangements of true leaves among the three species well because of their similarities of the shapes and arrangement (Figure 1). A comparison of the location of the output bounding box between detection success in patterns A and B and misrecognition as *S. angulatus* in C and D revealed no clear differences (Supplementary Figure S1). This suggests that detectors focused on similar parts in the image as the features of each species. Stage 3 (only true leaves) was treated as a single class in both patterns C and D. Treating similar shapes of different species as a class and training them with the same model may increase the risk of misrecognition. One way to avoid such issues is limiting targets, as observed in two-species models. For example, in two-species models excluding *I. lacunosa* and *S. angulatus*, misrecognition in patterns C and D did not occur, leading to increased detection success for true leaves of *I. coccinea* (Figure 4). However,

https://doi.org/10.1017/wsc.2024.63 Published online by Cambridge University Press

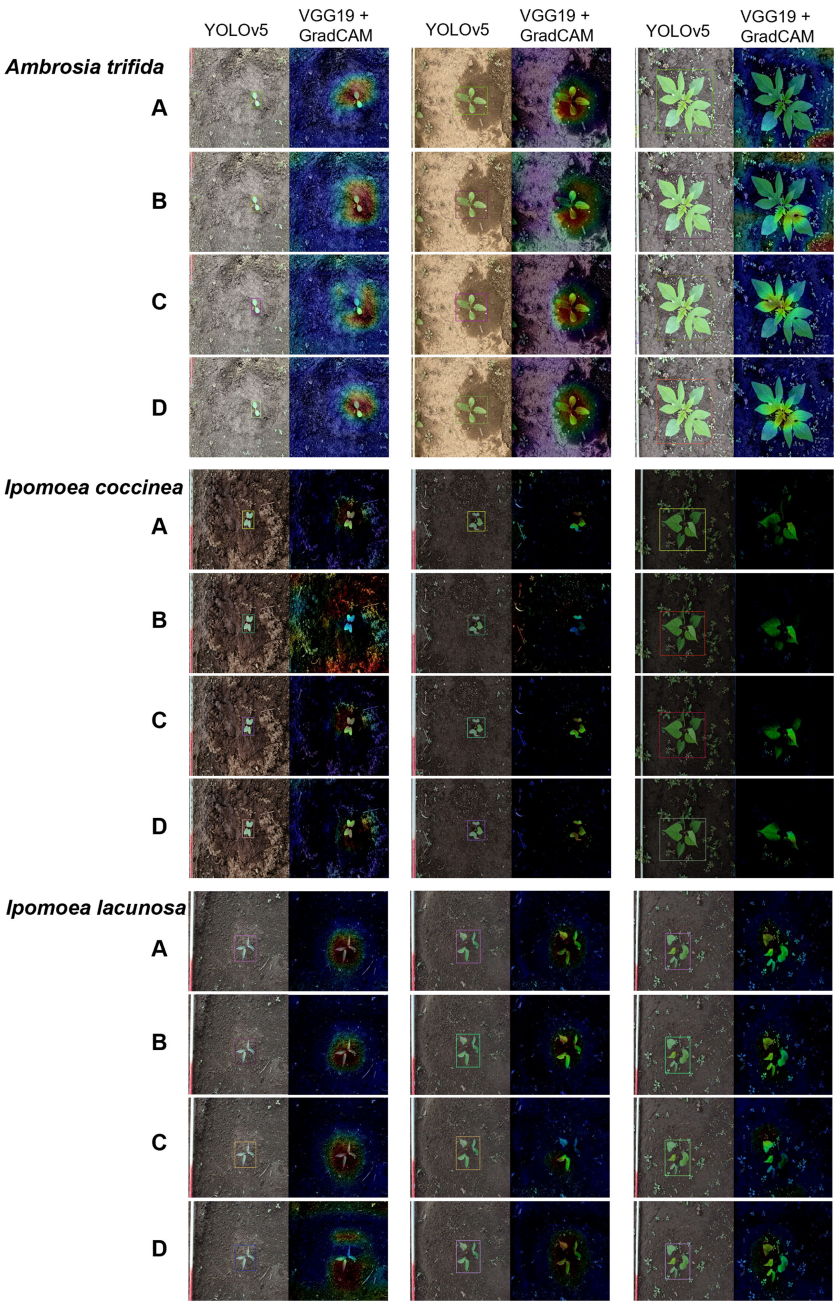


Figure 6. Examples from Evaluation 2 of You Look Only Once [YOLO] v5–based detection and gradient-weighted class activation mapping (GradCAM)-generated heat maps indicating Visual Geometry Group [VGG] 19–based classification. Note that *Sicyos angulatus* was not used in Evaluation 2, because its cultivation is not permitted in Japan.

misrecognition may occur in two-species models when nontarget species resembling the target species are apparent. Our results suggest the potential of another approach, wherein merging different growth stages with different shapes as a class, as observed in patterns A and B, can effectively prevent misrecognition (Figure 4). Although cotyledons and true leaves have distinct shapes in this study's target species, their integration is expected to contribute to maintaining stable recognition success at the species level during the early growth period.

Rates of NONDETECT tended to be higher in both four- and two-species models when leaf numbers were 2.5 to 4 (Figure 4). A leaf number of 2.5 indicates that true leaves were half-grown, whereas 3 or 4 corresponds to Stage 2 (cotyledons and one or two true leaves). These timings corresponded with changes in leaf shapes from cotyledons to true leaves. The timing of leaf shape changes may have increased training difficulty, although the number of training images categorized into Stage 2 was equal to that in Stages 1 and 3.

Results of recognition success under VGG19 did not exhibit a common pattern among target species (Figure 5; Supplementary Table S1). Rates of TRUE classification in two-species models were higher than those in four-species models. In four-species models, *A. trifida* was prone to misclassification as *I. coccinea* or *I. lacunosa*, with *I. coccinea* often misclassified as *I. lacunosa* and vice versa. GradCAM-generated heat maps illustrating classification success under VGG19 tended to focus on the whole plant shape or around the plant (Figure 6). However, heat maps of some images did not focus on target plants, despite successful classification. Thus,

https://doi.org/10.1017/wsc.2024.63 Published online by Cambridge University Press

over-learning may have occurred. Common patterns and biases in such heat maps were not discernible.

The Evaluation 2 results indicate that recognition accuracy was unstable during the early growth stage when leaf shapes changed temporally. However, they also suggest that integrating classes per species has the potential to increase accuracy, as observed for *I. coccinea* in four-species models under YOLOv5. For distinguishing among weed species with similar shapes and facilitate practical SSWM, merging different growth stages with different shapes as a single class, as demonstrated in patterns A and B, is effective.

When developing identifiers for specific plant species, determining how to train the temporal change in plant shape is a primary challenge. The present study reveals that integrating different shapes within a plant species as a single class is effective for maintaining robust recognition success during the early growth stage. This finding is expected to contribute not only to the early detection of weed seedlings but also to the robustness of general plant species identifications. Our study also highlights the difficulty of identifying multiple species and each growth stage simultaneously. As both pieces of information are essential for optimizing weed management and reducing herbicide use, solving this problem will enhance the application of image recognition technology to weed management. Although this issue is challenging, further technological improvements and the accumulation of training images are anticipated to address it in the future.

Supplementary material. To view supplementary material for this article, please visit https://doi.org/10.1017/wsc.2024.63

Acknowledgments. The authors thank T. Takayama for his support in setting up model environments; Y. Akamatsu, M. Asai, H. Asami, M. Fukuda, N. Ihara, S. Jingu, T. Kanno, Y. Kowata, H. Ohdan, N. Ueda, K. Sasaki, O. Watanabe, and N. Yoshino for their help in data collection; K. Ikeda for her help in annotation; and A. Kozaki for her support in cultivation. This research used the SHIHO supercomputer at NARO to train deep neural network models.

Funding statement. This study was supported by Research Project for Technologies to Strengthen the International Competitiveness of Japan's Agriculture and Food Industry.

Competing interests. The authors declare that there are no conflicts of interest.

References

Barnhart IH, Lancaster S, Goodin D, Spotanski J, Dille JA (2022) Use of open-source object detection algorithms to detect Palmer amaranth (*Amaranthus palmeri*) in soybean. Weed Sci 70:648–662

Coleman GRY, Bender A, Hu K, Sharpe SM, Schumann AW, Wang Z, Bagavathiannan MV, Boyd NS, Walsh MJ (2022) Weed detection to weed recognition: reviewing 50 years of research to identify constraints and opportunities for large-scale cropping systems. Weed Technol 36:741–750

Espejo-Garcia B, Mylonas N, Athanasakos L, Fountas S, Vasilakoglou I (2020) Towards weeds identification assistance through transfer learning. Comput Electron Agric 171:105306

Gildenblat J (2021) PyTorch Library for CAM Methods. https://github.com/jacobgil/pytorch-grad-cam. Accessed: January 23, 2024

Grey TL, Raymler P (2002) Sicklepod (*Senna obtusifolia*) and red morningglory (*Ipomoea coccinea*) control in glyphosate-resistant soybean with narrow rows and postemergence herbicide mixtures 1. Weed Technol 16:669–674

Hasan ASMM, Sohel F, Diepeveen D, Laga H, Jones MGK (2021) A survey of deep learning techniques for weed detection from images. Comput Electron Agric 184:106067

Huang H, Deng J, Lan Y, Yang A, Deng X, Zhang L (2018) A fully convolutional network for weed mapping of unmanned aerial vehicle (UAV) imagery. PLoS ONE 13: e0196302

Hussain MI, Abideen Z, Danish S, Asghar MA, Iqbal K (2021) Integrated weed management for sustainable agriculture. Sustain Agric Rev 52:367–393

Jocher G (2020) YOLOv5 by Ultralytics. https://github.com/ultralytics/yolov5. Accessed: January 23, 2024

Kurokawa S (2017) Alien weeds in agricultural land: problems and solutions. J Weed Sci Technol 62:36–47. Japanese

Kurokawa S, Hajika M, Shibuya T (2015) Canopy height-to-row spacing ratio as a simple and practical onsite index to determine the time for terminating *Ipomoea coccinea* control in the Japanese soybean-growing systems. Weed Biol Manag 15:113–121

Lee SR, Son DC (2022) Genetic diversity pattern reveals the primary determinant of burcucumber (*Sicyos angulatus* L.) invasion in Korea. Front Plant Sci 13:1–16

Lin T, Maire M, Belongie S, Bourdev L, Girshick R, Hays J, Perona P, Ramanan D, Zitnick CL, Dollár P (2014) Microsoft COCO: common objects in context. Pages 740–755 in Proceedings of the 13th European Conference on Computer Vision, Part V. Zurich, Switzerland: European Conference on Computer Vision.

López-Granados F (2011) Weed detection for site-specific weed management: mapping and real-time approaches. Weed Res 51:1–11

Lottes P, Behley J, Chebrolu N, Milioto A, Stachniss C (2018) Joint stem detection and crop-weed classification for plant-specific treatment in precision farming. Pages 8233–8238 *in* 2018 IEEE/RSJ International Conference on Intelligent Robots and Systems (IROS). Madrid, Spain: IEEE

Ministry of the Environment, Ministry of Agriculture, Forestry and Fisheries (2015) The List of Alien Species That May Have Adverse Effects on Ecosystems in Japan. https://www.env.go.jp/nature/intro/2outline/iaslist.html. Accessed: January 23, 2024. Japanese

Norsworthy JK, Oliveira MJ (2007) Effect of tillage and soyabean on *Ipomoea lacunosa* and Senna obtusifolia emergence. Weed Res 47:499–508

Partel V, Charan Kakarla S, Ampatzidis Y (2019) Development and evaluation of a low-cost and smart technology for precision weed management utilizing artificial intelligence. Comput Electron Agric 157:339–350

Rai N, Zhang Y, Ram BG, Schumacher L, Yellavajjala RK, Bajwa S, Sun X (2023) Applications of deep learning in precision weed management: a review. Comput Electron Agric 206:107698

R Core Team (2023) R: A Language and Environment for Statistical Computing. https://www.R-project.org. Accessed: January 23, 2024

Regnier EE, Harrison SK, Loux MM, Holloman C, Venkatesh R, Diekmann F, Taylor R, Ford RA, Stoltenberg DE, Hartzler RG, Davis AS, Schutte BJ, Cardina J, Mahoney KJ, Johnson WG (2016) Certified crop advisors' perceptions of giant ragweed (*Ambrosia trifida*) distribution, herbicide resistance, and management in the corn belt. Weed Sci 64:361–377

Rydahl P (2003) A web-based decision support system for integrated management of weeds in cereals and sugarbeet. EPPO Bull 33:455–460

Savić A, Oveisi M, Božić D, Pavlović D, Saulić M, Schärer HM, Vrbničanin S (2021) Competition between *Ambrosia artemisiifolia* and *Ambrosia trifida*: is there a threat of a stronger competitor? Weed Res 61:298–306

Selvaraju RR, Cogswell M, Das A, Vedantam R, Parikh D, Batra D (2020) Grad-CAM: visual explanations from deep networks via gradient-based localization. Int J Comput Vis 128:336–359

Smeda RJ, Weller SC (2001) Biology and control of burcucumber. Weed Sci 49:99–105

Sujaritha M, Annadurai S, Satheeshkumar J, Kowshik Sharan S, Mahesh L (2017) Weed detecting robot in sugarcane fields using fuzzy real time classifier. Comput Electron Agric 134:160–171

Teimouri N, Dyrmann M, Nielsen PR, Mathiassen SK, Somerville GJ, Jørgensen RN (2018) Weed growth stage estimator using deep convolutional neural networks. Sensors 18:1–13

Tzutalin (2015) LabelImg. https://github.com/HumanSignal/labelImg. Accessed: January 23, 2024

Wang A, Zhang W, Wei X (2019) A review on weed detection using ground-based machine vision and image processing techniques. Comput Electron Agric 158:226–240